minerals

MDPI

Article

Feasibility of a Mineral Carbonation Technique Using Iron-Silicate Mining Waste by Direct Flue Gas CO_2 Capture and Cation Complexation Using 2,2′-Bipyridine

Javier F. Reynes *, Guy Mercier, Jean-François Blais and Louis-César Pasquier

Institute National de la Recherche Scientifique (Centre Eau, Terre et Environnement), Université du Québec, 490 rue de la Couronne, Québec, QC G1K 9A9, Canada; guy.mercier@ete.inrs.ca (G.M.); jean-francois.blais@ete.inrs.ca (J.-F.B.); louis-cesar.pasquier@ete.inrs.ca (L.-C.P.)

* Correspondence: javier.fernandez_reynes@ete.inrs.ca; Tel.: +1-346-7733-5087

Abstract: Mineral carbonation is gaining increasing attention for its ability to sequester CO_2. The main challenge is doing it economically and energy-efficiently. Recently, many studies have focused on the aqueous reaction of carbon dioxide with the alkaline earth minerals such as serpentine, Mg-rich olivine and wollastonite. Nevertheless, Fe-rich olivines have been poorly studied because of their high energy demand, which make them unfeasible for industrial implementation. This article describes the feasibility of an indirect mineral carbonation process using silicic, Fe-rich mining waste with direct flue gas CO_2 via iron complexation using 2,2′-bipyridine. The overall process was performed in three main steps: leaching, iron complexation, and aqueous mineral carbonation reactions. The preferential parameters resulted in a recirculation scenario, where 38% of Fe cations were leached, complexed, and reacted under mild conditions. CO_2 uptake of 57.3% was achieved, obtaining a Fe-rich carbonate. These results are promising for the application of mineral carbonation to reduce CO_2 emissions. Furthermore, the greenhouse gas balance had a global vision of the overall reaction's feasibility. The results showed a positive balance in CO_2 removal, with an estimated 130 kg CO_2/ton of residue. Although an exhaustive study should be done, the new and innovative mineral carbonation CO_2 sequestration approach in this study is promising.

Keywords: mineral sequestration of CO_2; carbon dioxide; global warming; mine waste; iron carbonate; 2,2′-bipyridine

Citation: Reynes, J.F.; Mercier, G.; Blais, J.-F.; Pasquier, L.-C. Feasibility of a Mineral Carbonation Technique Using Iron-Silicate Mining Waste by Direct Flue Gas CO_2 Capture and Cation Complexation Using 2,2′-Bipyridine. *Minerals* **2021**, *11*, 343. https://doi.org/10.3390/min11040343

Academic Editor: Rafael Santos

Received: 27 January 2021
Accepted: 24 March 2021
Published: 26 March 2021

1. Introduction

The reduction of greenhouse gas (GHG) emissions is a major environmental challenge given their negative impact on the ecosystem. The Intergovernmental Panel for Climate Change (IPCC) has reported an increase in the average global temperature of about 0.91 °C between 1880 and 2015, with an estimated increase rate of 0.2 °C per decade, caused mainly by anthropogenic GHG emissions [1] an increase in the average global temperature of about 0.85 °C between 1880 and 2012, with an estimated increase rate of 0.2 °C per decade, caused mainly by anthropogenic GHG emissions. This temperature increase has caused changes in the global climate, with serious consequences for humans and ecosystems, including more extreme weather, droughts, polar ice melting, increased sea levels, and increased ocean acidification [2–5].

Policymakers expect that limiting the temperature increase to 1.5 °C above pre-industrial levels, as opposed to 2 °C or more, will ensure that global climate change remains reversible. Global anthropogenic CO_2 emissions would consequently need to decrease by 45% from 2010 levels by 2030, reaching "net zero" by 2050 [6]. In 2008, Quebec entered the Western Climate Initiative along with other Canadian provinces (British Columbia, Manitoba, and Ontario) and California (USA) to implement a cap and trade system to reduce GHG emissions [7]. Since 2013, industries with high CO_2 emissions have

been subject to GHG emission regulations to avoid carbon taxes. Consequently, these industries must find solutions to reduce their emissions [8].

CO_2 capture and storage or utilization methods for reducing GHG emissions are gaining increasing attention to reduce post-combustion gaseous emissions. Both of these methods involve CO_2 capture from industrial emissions and its transport in a pipeline or by ship. This CO_2 could be stored geologically or biologically (e.g., CO_2 capture and storage) or reused by transforming it into a product with sale value [9–11]. In particular, mineral carbonation is fast becoming an important method of removing CO_2 and obtaining carbonates with potential sale value. This reaction involves a chemical reaction between CO_2 and divalent metals (Ca, Mg, Fe or Ba) to form stable reusable carbonates [12]. Mineral carbonation is thermodynamically favorable but kinetically slow, and its reaction rate should be increased to make its application feasible at an industrial scale [13].

Mineral carbonation was originally proposed by Seifritz [14]. Subsequently, the concept of binding CO_2 in Ca and Mg carbonate minerals was proposed by Dunsmore [15], and additional investigations were done by Lackner et al. [16,17] More recently, several reports on CO_2 sequestration by mineral carbonation have been published, with particular focus on four minerals: Mg-rich olivine (forsterite, Mg_2SiO_4); [18–22], serpentine ($Mg_2Si_2O_5(OH)_4$); [23–26], wollastonite ($CaSiO_3$); [27,28] and Basalt [29–31]. Few studies have used Fe-rich silicates, and the studies that did usually focused on aqueous mineral carbonation using supercritical and anoxic conditions for CO_2 or high reaction conditions that are not competitive for application at an industrial scale because of the amount of energy required [32–34]. Most studied mineral carbonation reactions were performed in aqueous media because of the low reaction kinetics of the gas phase reaction under dry conditions [35]. Indirect mineral carbonation reactions, where divalent cations are extracted into the solution prior to the reaction with CO_2, have much better reaction efficiencies and are thus more suitable for future industrial implementation, even more with refractory materials [36].

This study focused on providing a solution to Fe-rich silicate mining residue from Mine Arnaud, an apatite mine in the Sept-Îles, QC, Canada [37]. The residue is mainly composed of silicates, particularly, Fe-rich olivine (fayalite, Fe_2SiO_4) with approximately 16% Fe and 19% Si. With 81.2 Mt CO_2-eq, GHG emissions from Quebec represent 11.2% of Canada's total emissions [38]. Due to hydroelectricity, transportation and industries represent the major emitters with industrial clusters in the province emitting most of the GHGs [39]. One such area is situated in the area of Sept-Îles and Port-Cartier with ArcelorMittal iron pellet plant and Aluminerie Alouette aluminum manufacturing plant, the CO_2 emissions of which are 863 and 1.12 Mt CO_2-eq/year, respectively. These industries are adjacent to Mine Arnaud, and mineral carbonation is an ideal way for removing CO_2 from industrial gases and reusing Fe-rich mining residue.

The main problem with Fe-rich carbonate precipitation is the stabilization of iron (II) cations in under alkaline pH conditions without forming undesired iron hydroxide precipitates [40]. In the Eh-pH diagram of iron species [41], hydroxide precipitation starts at around pH 6, whereas that of $FeCO_3$ occurs between pH 9 and pH 12. This problem is proposed to be solved by using 2,2′-bipyridine as a ligand, forming $[Fe(bipy)_3]^{2+}$, a very stable iron (II) complex that avoids the undesired precipitation of other iron compounds.

The indirect mineral carbonation process proposed in this study consisted of three main steps. First, a leaching process was performed using ammonium bisulphate (NH_4HSO_4) as an acid solvent to extract Fe and Mg cations in solution. Second, since a basic pH (9–12) was necessary for the mineral carbonation reaction, sodium hydroxide (NaOH) was used and Fe complexation using 2,2′-bipyridine was done to avoid the precipitation of Fe hydroxide [42]. Third, CO_2 gas was added to the solution to obtain the final carbonate. It is important to note that the 2,2′-bipyridine and NH_4HSO_4 remains in solution during the process, they are regenerated and released after the mineral carbonation reaction when the CO_2 is added.

Equations (1)–(5) show the series of reactions that take place in the aqueous mineral carbonation present in this work:

$$(Fe, Mg, Ca)_2SiO_4 + 4NH_4HSO_4 \leftrightarrow 2(Fe, Mg, Ca)SO_{4(aq)} + 2(NH_4)_2SO_{4(aq)} + SiO_2 + 2H_2O \quad (1)$$

$$(Fe, Mg, Ca)SO_{4(aq)} + 3(2,2' - bipyridine)^{2+} + H_2O + NaOH_{(aq)} \leftrightarrow [Fe(bipy)_3]^{2+} + (Mg, Ca)SO_{4(aq)} + H_2O + NaOH_{(aq)} \quad (2)$$

$$CO_{2(g)} + H_2O \leftrightarrow H_2CO_{3(aq)} \leftrightarrow HCO_3^- + H^+ \leftrightarrow CO_3^{2-} + H^+ \leftrightarrow +NH_3{\cdot}H_2O \leftrightarrow NH_4HCO_{3(aq)} \quad (3)$$

$$[Fe(bipy)_3]^{2+} + (Mg, Ca)SO_{4(aq)} + 2NH_4HCO_{3(aq)} + 2H_2O + NaOH_{(aq)} \leftrightarrow (Fe, Mg, Ca)CO_{3(s)} + (NH_4)_2SO_{4(aq)} + 3(2,2' - bipyridine)^{2+} + 2H_2O + NaOH_{(aq)} + HCO_3^- \quad (4)$$

$$(NH_4)_2SO_{4(aq)} \leftrightarrow NH_4\,HSO_4 + NH_{3(g)} \quad (5)$$

As the main mineral present in the residue is the fayalite. The overall reaction of its mineral carbonation can be described as Equation (6):

$$Fe_2SiO_4 + 2CO_2 + 2H_2O \rightarrow 2FeCO_3 + SiO_2 + 2H_2O + 90\ kJ/mol \quad (6)$$

This study is focused on providing a solution to Fe-rich silicate mining residue from Mine Arnaud, an apatite mine in the Sept-Îles, QC, Canada [37]. The residue is mainly composed of silicates, particularly, Fe-rich olivine (fayalite, Fe_2SiO_4) with approximately 16% Fe and 19% Si. The feasibility of an indirect mineral carbonation reaction via Fe complexation using, Fe-rich silicates mining residues to reduce CO_2 emissions from industrial flue gases have been studied. A recirculation scenario was optimized for reusing and valorizing the reagents and products to reduce the costs and increase the feasibility of future industrial implementation. GHG estimations were performed, but exhaustive analyses at even larger scales need to be done. The results of this study revealed potential sensitivities regarding the future industrial implementation of the proposed mineral carbonation approach in the Sept-Îles region.

2. Materials and Methods

2.1. Materials

For this study, silicate mining residues collected from Mine Arnaud were used as a source of cations extracted by a leaching process using NH_4HSO_4 (≥99.5%, Acros Organics, Geel, Belgium) as the acid leaching agent. Residues were received, homogenized, and characterized prior to use [37]. Then, 2,2′-bipyridine (≥99%; Sigma-Aldrich, St. Louis, MO, USA, ReagentPlus®) was used to obtain an $[Fe(bipy)_3]^{2+}$ red complex. Pure ethanol (≥99%; Fisher Chemical, Hampton, NH, USA) was used to facilitate the aqueous dissolution of the ligand. NaOH (≥97.0%; ACS Reagent, Washington, DC, USA) was used as a buffer solution. Two CO_2 gas cylinders, one with 10 wt.% CO_2 (mean cell residence time; CO_2 10% N2 Bal 200SZ Certified; Linde Group, Dublin, Ireland) and the other with pure CO_2 (CO_2 Industrial Grade, UN1013; Linde Group, Dublin, Ireland), were used. Deionized water was used to prepare the solutions in all the experiments.

2.2. Synthesis

Different stock solutions were prepared for mineral carbonation. First, a 1.5 M NH_4HSO_4 solution (172.7 g NH_4HSO_4 in 1000 mL deionized water) was prepared. Then, the $[Fe(bipy)_3]^{2+}$ complex was obtained by mixing 20 mL of the leachate with 28.5 mL of a 2,2′-bipyridine 0.05 M stock solution prepared by mixing 7.80 g 2,2′-bipyridine in a 1000 mL mixture of ethanol (120 mL) and deionized water (880 mL). Once the complex was obtained, a 1 M NaOH buffer solution (40 g NaOH (s) pellets in 1000 mL deionized water) was used to achieve the required pH at which the reaction was performed. Finally, CO_2 (g) was added to the basic complex solution. For each recirculation, 20 mL of the leaching solution was added. The solid carbonates obtained were filtrated and dried at 60 °C for 24 h for characterization.

2.3. Analytical Methods

Mine Arnaud extracts apatite and generates a silicate residue that was received, homogenized, and characterized prior to its use in this study. The material did not need to be crushed, because the median particle size of the residue was 65 µm, which was optimal for performing mineral carbonation [43]. An inductively coupled plasma–optical emission spectrometry (ICP-OES) analysis (Varian ICP-OES Spectrometer 725-ES, Palo Alto, CA, USA) was used

to determine the chemical composition of the solid and liquid samples. Solid samples were fused with Li metaborate (Corporation Scientifique Claisse, Québec, QC, Canada) prior to ICP analysis. Inorganic carbon analysis was performed with an inorganic carbon analyzer (Shimadzu TOC-V CPH, Tokyo, Japan) for liquid samples and with a carbon, hydrogen, nitrogen, sulfur analyzer (Leco TruSpec Micro, St Joseph, MI, USA) for solid samples. All pH measurements were performed using a Fisher Scientific Accumet AR25 pH meter. An Isotemp oven (Fisher Scientific 737F, Waltham, MA, USA) and an analytical laboratory balance (Sartorius Quintix 224-1S, Wood Dale, IL, USA) were also used to dry and weight the carbonates obtained.

2.4. Methods

This section details all the stages of the experiments: Characterization of the $[Fe(bipy)_3]^{2+}$ and regeneration of the 2,2′-bipyridine, the leaching stage, the mineral carbonation successive batch reactions to optimize the parameters and study the ligand (2,2′-bipyridine) recovery potential, and the final recirculation scenario of the mineral carbonation experimental design.

2.4.1. Characterization of the $[Fe(bipy)_3]^{2+}$ and Regeneration of the 2,2′-Bipyridine

In order to confirm the mechanism of the mineral carbonation reaction through the formation of the $[Fe(bipy)_3]^{2+}$ complex and the 2,2′-bipyridine regeneration Equations (1)–(5), the time-dependent IR-spectra of the 2,2′-bipyridine before its complexation with iron cations Equation (2) and after the formation of iron carbonates where the 2,2′-bipyridine has already been complexed Equation (4) were recorded within 3800–500 cm^{-1} in the transmission mode at ambient temperature and pressure, showing the spectra as transmittance.

2.4.2. Leaching Process and Valorization of the Mining Residue

Leaching of the mining residue to extract the cations was the first step of the indirect mineral carbonation approach, and 40 g of the previously dried residue was mixed with 200 mL of the previously prepared 1.5 M NH_4HSO_4 solution in an Erlenmeyer flask. The flask was closed to avoid mass loss by evaporation and placed in a water bath at a temperature of 61 °C and stirring speed of 250 rpm for a reaction time of 2 h. These parameters were studied and optimized prior to the present study. Furthermore, NH_4HSO_4 was the most suitable solvent because it does not interfere with other reagents but produces good reaction yields, has low toxicity, and has a high recovery potential [44].

An important objective of the proposed mineral carbonation approach was to find a way of reusing and valorizing mining residue from Mine Arnaud. The first leaching batch had an efficiency of about 30 wt.% and 50 wt.% for Fe and Mg, respectively, and a large proportion of the cations remained in the solid. Furthermore, the solid was not wholly inert, and the storage problem (an objective of the mineral carbonation) could not be solved. Three successive leaching batches were performed to compare their stability and study the purity of the final product and its possible valorization.

2.4.3. Mineral Carbonation Reaction: 2,2′-Bipyridine Recovery Potential and Preferential Reaction Conditions in Recirculation Scenario

Once the leaching process had finished, a stoichiometric amount of leachate was mixed with the 1.5 M 2,2′-bipyridine stock solution to form a $[Fe(bipy)_3]^{2+}$ red complex. The experimental setup in the recirculation scenario is shown in Figure 1.

All reactions were done using a three-neck round bottomed flask so that the pH and temperature could be controlled. Four different pH levels, from 9 to 12, and three temperatures (21, 60, and 80 °C) were tested, and the stirring speed was fixed at 250 rpm. Two gas mixtures of 10 wt.% and pure CO_2, respectively, were used. Once the conditions were set, the gas was injected into the solution at a rate of 1.5 L/min. Reactions were performed under atmospheric pressure in order to decrease the energetic requirements. Samples were taken at 30, 60, and 120 min. After a reaction time of 2 h, the obtained product was filtered, separating the carbonate (solid phase) from the recovered liquid. The liquid phase was reintroduced into the flask with

20 mL of the initial leachate to assure 100% complexation and to compare all the parameters under the same reaction conditions; the minimum amount of NaOH was added to increase the pH. Three reactions were performed for each experimental condition. Different analyses were performed to characterize the liquid phase (total inorganic carbon, total organic carbon, and ICP-OES) and solid phase (X-ray diffraction and carbon, hydrogen, nitrogen, sulfur), to study the recovery potential of the ligand, and to obtain the most favorable and most stable reaction conditions in a recirculation scenario.

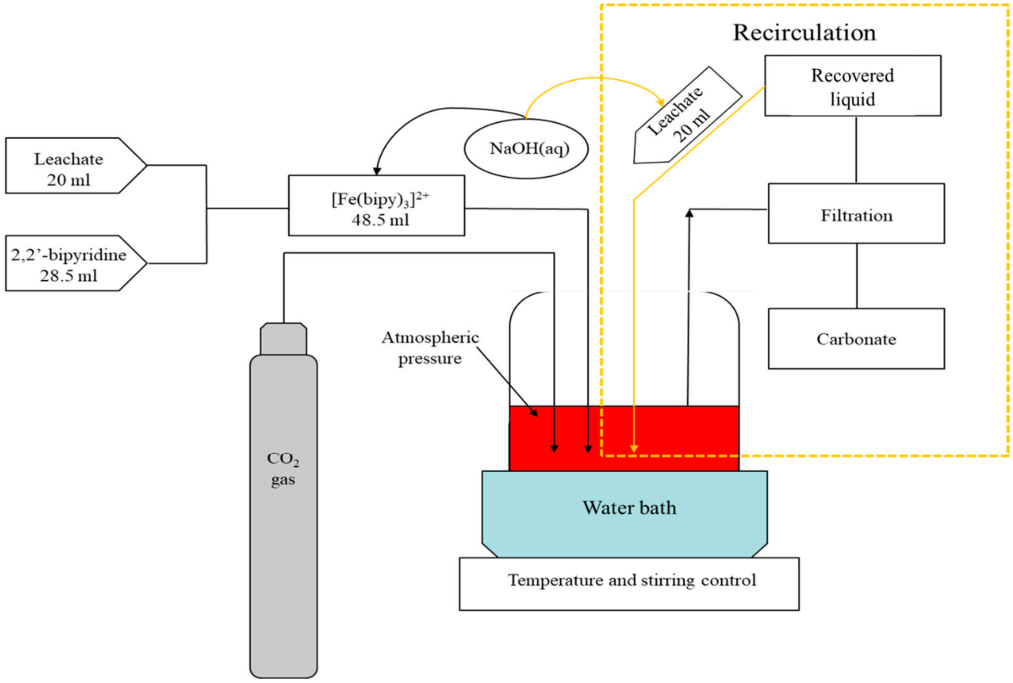

Figure 1. Schematic presentation of experimental setup.

2.4.4. Global Evaluation of Mineral Carbonation Approach

The mineral carbonation approach was tested in a recirculation scenario using the optimized conditions. The global experimental design is presented in Figure 2.

To leach 4 g of the initial mining residue, 20 mL NH_4HSO_4 were used. The obtained leachate was mixed with 28.5 mL 2,2′-bipyridine (dissolved with the minimum amount of ethanol) to complex the Fe and obtain 48.5 mL $[Fe(bipy)_3]^{2+}$ acid complex solution. Then, the pH was increased using NaOH, and the temperature and stirring speed were set at the optimum conditions obtained previously (see Section 3.2). The 10 wt.% CO_2 gas stream was injected at a rate of 1.5 L/min for a reaction time of 2 h, imitating a real industrial gas mixture. The resulting product was filtered, separating the solid phase containing the carbonate and the liquid phase containing the recovered liquid, the NH_4HSO_4 that is regenerated after the reaction Equation (5) and the 2,2′-bipyridine that was previously complexed with the Fe that is released and reused for the recirculation process (Equation (4)). The solid was then dried for analysis. As the recovered liquid phase had a final pH of 7–8 due to the carbonate ions present in the final solution and the fact that the NH_4HSO_4 is recovered after the mineral carbonation reaction, only 4 mL of a new NH_4HSO_4 solution were needed to decrease the pH to 1–2 to reuse it as leaching agent (instead of the 20 mL of NH_4HSO_4 that were used in the first reaction). Furthermore, after the first mineral carbonation reaction, the 2,2′-bipyridine is released into the solution with the recovered liquid and it can be reused again for the next mineral carbonation reaction Equation (4). Three recirculation reactions were performed. The partially reacted residue obtained in the first batch was mixed with the ones obtained in the following recirculation reactions. Samples of the liquid and solid phases were taken and analyzed, after which the overall efficiency of the mineral carbonation approach was determined.

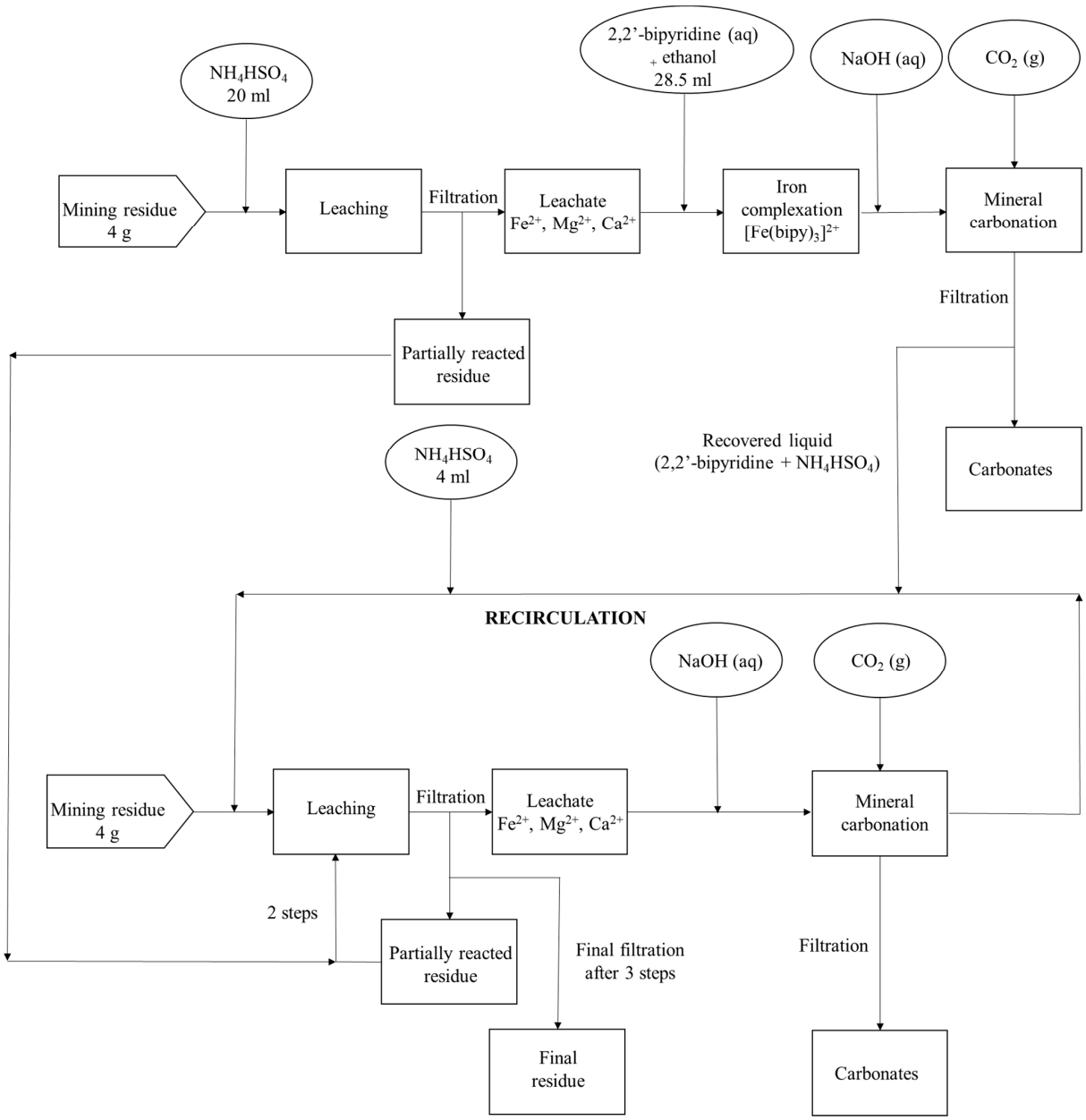

Figure 2. Conceptual process scheme for producing Fe carbonates from Mine Arnaud mining residues. Numbers are based on experimentally verified results.

2.4.5. GHG and Mass Balance

The mass and GHG balance have been estimated. The mass balance have been done using a block flow diagram where all the inlet and outlet streams have been calculated. The GHG balance was calculated based on GHG emission factors and energy requirements. Transportation emission factors were taken from the World Resource Institute's *GHG Protocol: Corporate Accounting and Reporting Standard* GHG calculation tool ver. 2.6 (2011). Emissions factors for the energy use of the leaching and mineral carbonation reaction plant were obtained from Natural Resources Canada for hydroelectric energy and natural gas [45].

3. Results and Discussion

3.1. Characterization of the $[Fe(bipy)_3]^{2+}$ and Regeneration of the 2,2′-Bipyridine

Figure 3 shows the spectrum corresponding to 2,2′-bipyridine before its complexation with iron cations Equation (2) and after the formation of iron carbonates where the 2,2′-

bipyridine has already been complexed Equation (4). Since the spectrum is similar, it has only been included once. Then, the IR spectra of $[Fe(bipy)_3]^{2+}$ complex solution was recorded (Figure 4). When 2,2′-bipyridine is complexed to a metallic ion such as iron, its IR spectrum changes particularly in the regions 1650–1400 cm^{-1} (C=N and C=C ring stretching vibrations) and 1050–850 cm^{-1} (C–N out-of-plane deformations) [46]. Comparing those peaks in both IR spectra, the formation of $[Fe(bipy)_3]^{2+}$ complex in the solution and the regeneration of the 2,2′-bipyridine can be confirmed. Note that the broad peak near 3300 cm^{-1} refers to water of crystallization.

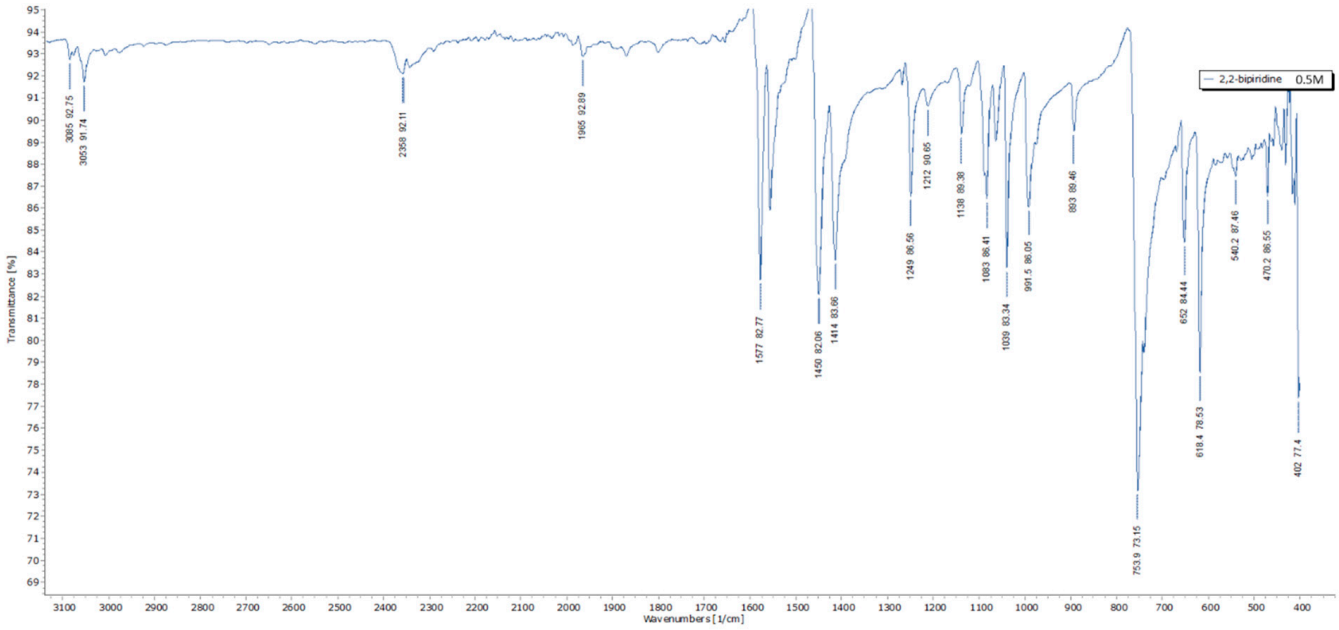

Figure 3. IR spectra of the 2,2′-bipyridine solution (0.5 M) before its complexation Equation (2) and after the mineral carbonation reaction Equation (4) at ambient temperature and pressure.

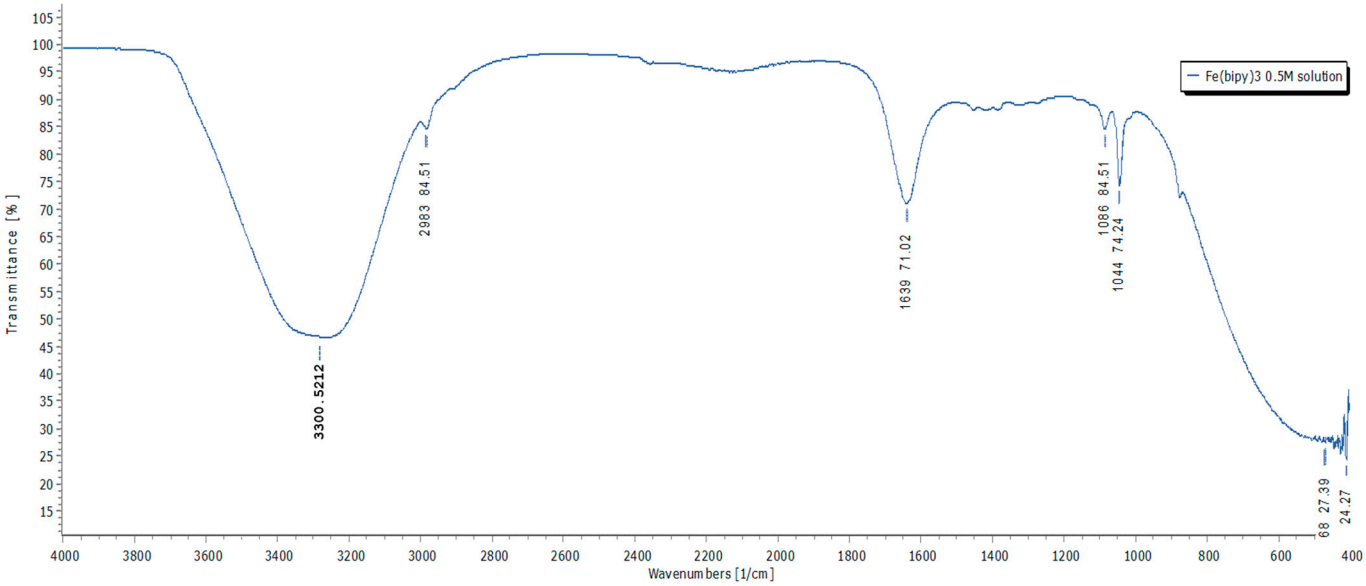

Figure 4. IR spectra of the $[Fe(bipy)_3]^{2+}$ complex solution (0.5 M) at its natural pH (3.27) and ambient temperature and pressure.

3.2. Optimization of Leaching Stage and Valorization of Residue

To evaluate the leaching efficiency, the chemical composition of the mining residue before and after leaching was calculated via ICP-OES. Table 1 shows the leaching composition of the mining residue before and after the first leaching reaction in mg/40 g of residue. The main elements leached were Fe (29%), Mg (40%), and Si (10%) from the olivine mineral phase. The amount of leached Ca (in the form of anorthite, $CaAl_2Si_2O_8$) was negligible (around 5%). Eight leaching processes were simultaneously performed and analyzed to ensure the accuracy and precision of the results. The results showed a decrease in the amount of Fe and Mg leached in each successive batch, since each leachate had fewer ions available in the solid. The amount of Si leached also decreased significantly since the first leaching because of the destruction of the silicate crystalline structure (olivine) and the formation of amorphous silica (passivation layer of SiO_2), which was stable and did not release Si from its structure.

Table 1. Chemical composition of the mining residue and the leachate for the first leaching in mg/40 g of sample. Only major elements are presented.

Mining Residue before Leaching (mg/40 g of Sample)				
Sample	Ca(II)	Fe(II)	Mg(II)	Si(IV)
1	2449	6646	2334	8187
2	2525	6518	2318	8328
3	2460	6750	2369	8286
4	2442	6731	2357	8130
5	2405	6839	2347	8061
6	2503	6775	2366	8127
7	2476	6595	2336	8243
8	2397	6822	2355	8065
Mean	2457 ± 46	6710 ± 123	2348 ± 20	8178 ± 99
Leachate (mg/40 g of sample)				
Sample	Ca(II)	Fe(II)	Mg(II)	Si(IV)
1	130	2344	1276	1642
2	145	2344	1295	1659
3	146	2332	1262	1640
4	140	2329	1199	1660
5	160	2308	1278	1640
6	152	2303	1220	1691
7	136	2307	1291	1693
8	150	2380	1298	1624
Mean	145 ± 10	2331 ± 58	1264 ± 36	1656 ± 26

The leaching efficiency was then calculated (Figure 5a). The results showed that the Mg leaching efficiency was better than that of Fe because of the weaker covalent bonds of Mg in the structure compared to the metallic covalent bond formed with Fe. Regardless, since the amount of Fe (160 mg/g) was higher than that of Mg (57 mg/g) in the mining residue, more Fe was present in the leachate. Furthermore, Si decreased significantly (from 18 to 4%), making the remaining solid rich in silica.

Subsequently, the richness of Si in the remaining residue was calculated to determine its future valorization. Figure 5b displays the element composition of the remaining residue, showing that the solid had a silica (SiO_2) composition of 87.50%. Since the final residue had a high Si purity, a product that could be easily recovered and sold could be obtained, removing the problem of waste storage and acquiring an economic value that would reduce the total costs of mineral carbonation. In addition, since the solid also contained about 8% Fe_2O_3, it could be sold for the formation of ferrosilicon compounds, whose market value could be even higher [47,48]. Nevertheless, a more in-depth market study is necessary to determine the economic value that could be obtained from this product.

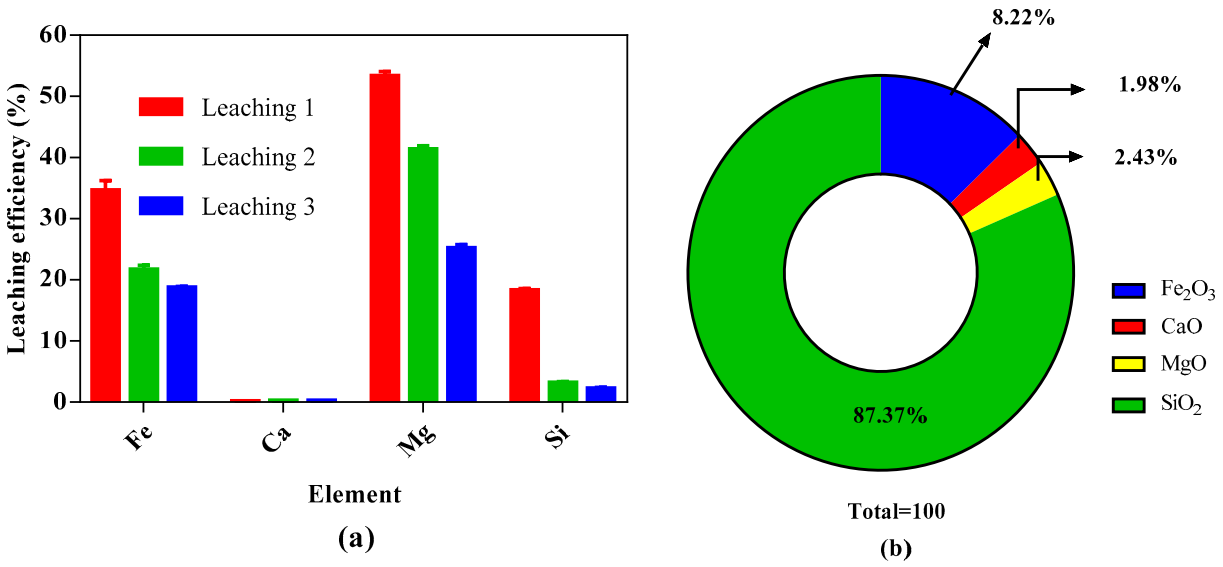

Figure 5. (**a**) Leaching efficiency (wt.%). Error bars indicate standard deviations, n = 3; (**b**) Element composition of residue obtained after final leaching process provided as oxides (%), n = 3.

After the first mineral carbonation batch performed, the resulting liquid was recirculated for further leaching stage in a recirculation scenario. The leaching efficiency after three recirculation reactions was performed to ensure that using the recovered liquid instead of a pure NH_4HSO_4 solution would not negatively affect the leachate and decrease the reaction efficiency. Figure 6 shows the leaching efficiency after each recirculation reaction for the cations of interest (Ca, Fe, Mg, and Si). The results showed an increase of about 10% in the reaction efficiency for Ca, Fe, and Mg between the leachate obtained using pure NH_4HSO_4 (1) compared with the essays performed with the recirculated solution (2 and 3). The cations aided the diffusion of inner-cations through the carrier pores to reach the solvent [49]. However, the amount of Si leached remained constant. After the first leaching process, the reaction efficiency stabilized, with average leaching results of 12, 38, 51, and 9% for Ca, Fe, Mg, and Si, respectively. Importantly, in addition to the good reaction efficiency, the amount of NH_4HSO_4 needed to decrease the pH of the recovered liquid (from 7 to 1–2) to make it suitable for leaching was 10 times less than that needed for the first leaching process with the pure acid solvent, decreasing the costs and rendering the process more profitable.

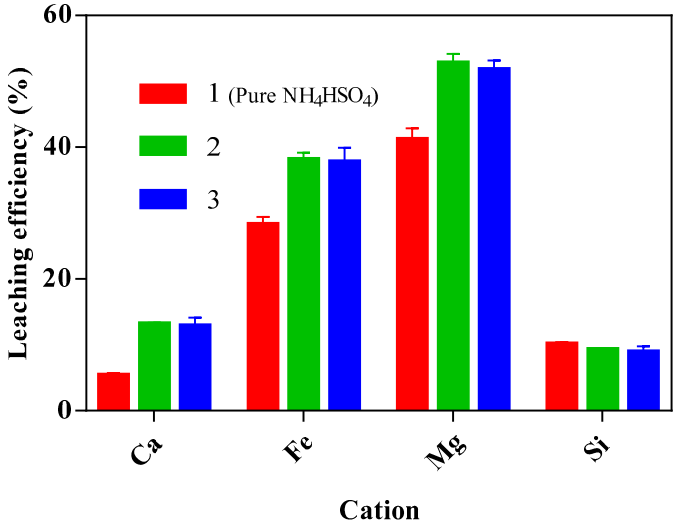

Figure 6. Leaching efficiency (%) for each cation in solution obtained for each recirculation reaction. Error bars indicate 5% error; n = 3.

3.3. Mineral Carbonation Reaction

3.3.1. Preferential Reaction Conditions in a Recirculation Scenario

When the leaching had finished and the ferrous cation (Fe^{2+}) had complexed with the 2,2′-bipyridine to yield the $[Fe(bipy)_3]^{2+}$ red complex, the next step of this approach was the mineral carbonation reaction. Temperature and pH dependence (Figure 7) were studied in a recirculation scenario to determine the preferential reaction conditions. The amount of 2,2′-bipyridine remained constant to determine its recovery potential, which was a limiting step because of the high cost of the ligand (USD 4930 for 1 ton). The amount of CO_2 uptake depended on two main factors: the CO_2 dissolved and instability of the complex. These two factors depend on temperature, and the pH only depends on the complex stability. While the amount of CO_2 dissolved increases at lower temperatures, the complex instability decreases at higher temperatures and pH, since the more energy is given to the system, the less stable the complex becomes.

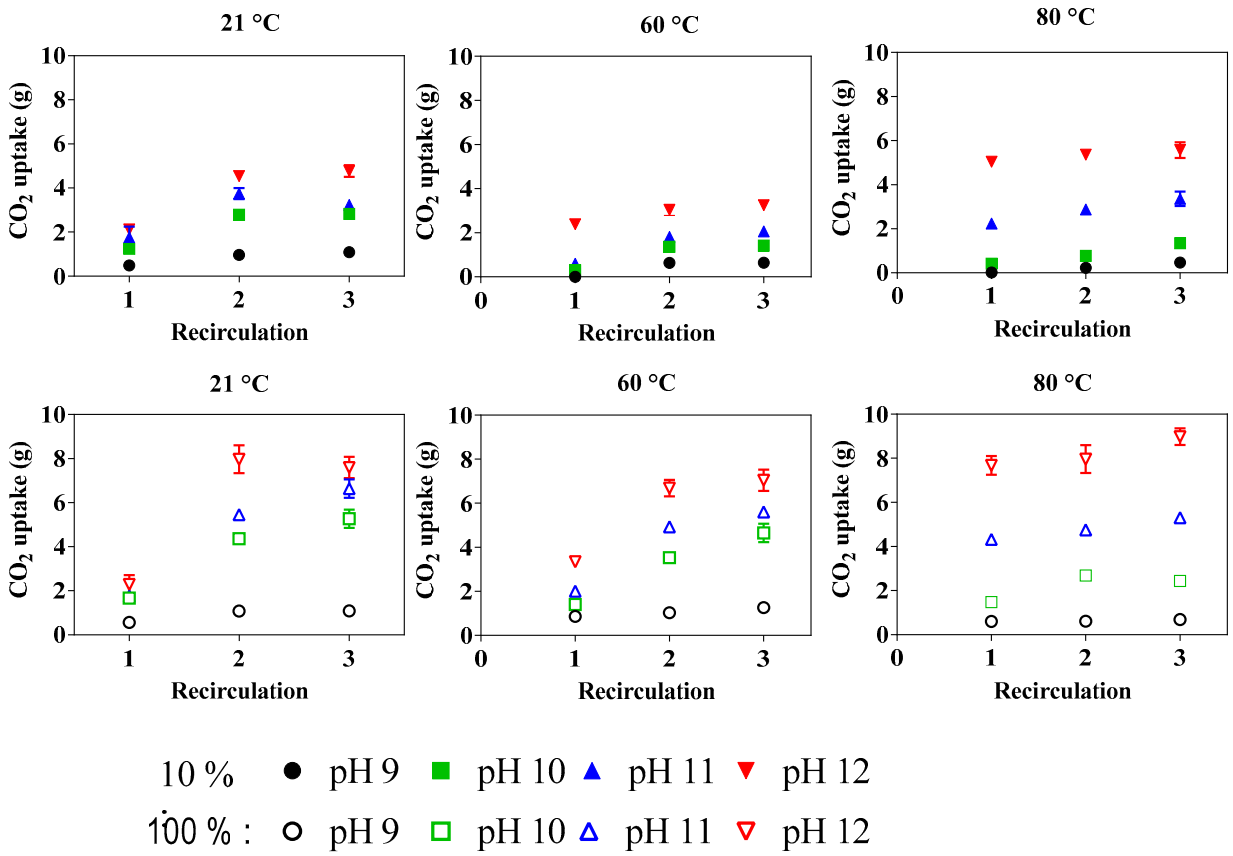

Figure 7. CO_2 uptake vs. recirculation reaction under each reaction condition (21, 60, and 80 °C) at pH 9–12 and CO_2 mixture of 10 and 100%, showing the effect of pH. Error bars indicate 5% error, n = 3. For some points, error bars are shorter than height of symbol.

CO_2 uptake is highly dependent on pH, especially at pH 12, because as mentioned above, complex destabilization. However, the dependence of CO_2 uptake on temperature is more complex, because both factors played an important role, and their effects were inversely proportional. The amount of CO_2 dissolved was high at 21 °C, and the results showed a higher amount of CO_2 uptake than that at 60 °C, a temperature at which the complex is still highly stable. Temperature is therefore a limiting factor for CO_2 dissolved at any pH, explaining the results obtained. At 80 °C, the same effect was observed at pH 9 and 10, where the results were better at lower temperature. When the reaction occurred at 80 °C and higher pH (11–12), the CO_2 uptake was much better than that observed at 21 °C. Therefore, under such conditions, the instability of the complex is the limiting factor

regardless of the effect of the CO_2 dissolved. Importantly, the amount of CO_2 uptake at a lower pH (9–10) was low and independent to temperature, indicating that pH had a stronger effect on reaction efficiency than temperature did. This can be explained because the complex stability only depends on pH and not on the CO_2 dissolved, as was true for temperature.

The recirculation reactions were compared to determine the most favorable reaction conditions and to establish whether the 2,2′-bipyridine could be totally reused. There was an inversely proportional temperature-dependence, showing a remarkable increase in reaction efficiency between the first and second recirculation reactions at 21 °C, which stabilized in the third recirculation. However, this effect decreased significantly as the temperature increased and was not observed at 80 °C because of the rapid destabilization of the complex at higher temperatures. Even the amount of CO_2 dissolved was lower at higher temperatures, best results were obtained at 80 °C. Furthermore, the increase of the total volume of the mineral carbonation reaction caused by the addition of NaOH and NH_4HSO_4 could be controlled by evaporation.

On the other hand, the amount of CO_2 uptake at higher pH (12) increased significantly, which yielded better results (by up to 50%) than that at pH 11. Finally, the use of pure CO_2 gave better results than that of 10 wt.% CO_2 gas streams did. Nevertheless, for the most favorable reaction conditions (pH 12 and 80 °C), the difference in CO_2 uptake in both cases was close, considering that it used 10 times less gas (5.68 vs. 8.84 g of CO_2 uptake at 10 and 100 vol.% CO_2, respectively). Moreover, considering that industrial gases have between 6 and 18 wt.% CO_2 gas [50], the most suitable conditions in terms of efficiency and feasibility (CO_2 uptake) were observed at 80 °C, pH 12, with a fixed stirring speed of 250 rpm, with a 10 wt.% CO_2 gas at an injection rate of 1.5 L/min, and at ambient pressure.

3.3.2. Carbonate Precipitation

The carbonate composition and morphology under each reaction condition were studied, and the element composition was stoichiometrically compared with the total inorganic carbon and carbon, hydrogen, nitrogen, sulfur results; the final product composition was calculated (Table 2). The carbonate purity varied between 68 wt.% and 78 wt.%, being slightly higher at lower temperatures and pH values. This could be explained by the amount of silica present in the sample and the higher amount of NaOH needed at higher pH. At lower temperatures and pH, the percentage of silica was higher and corresponded to the impurity of the carbonate in its entirety. As the temperature and pH increased, the opposite occurred, where the percentage of carbonate and silica decreased, evidencing the presence of another impurity, mainly from Na cations released by the NaOH solution. At higher temperatures the solubility of NaOH increases, resulting in higher Na concentration in the solution [51,52]. Consequently, its co-precipitation with the carbonate is higher, making the carbonate less pure.

Based on the amount of carbonate obtained, the percentage and ratio of Fe and Mg carbonate was calculated. The $FeCO_3$ purity decreased from an Fe/Mg ratio of 0.90 to 0.68 when the pH and temperature increased. Since the precipitation of Fe carbonate was favored because of the larger amount of Fe^{2+} cations in solution, the reaction efficiency was lower under milder conditions compared with that at higher temperature and pH, enabling the precipitation of purer Fe carbonate but in much lower quantities. To ensure that only Fe and Mg carbonates were obtained and that other possible impurities, such as Fe or Mg hydroxides, precipitated, the stoichiometry of the reaction was calculated, comparing the mol of Fe^{2+} and Mg^{2+} with that of CO_3^{2-} ions. The results showed that the ratio (mol Fe^{2+} + mol Mg^{2+})/mol CO_3^{2-} approached 1, verifying that all the Fe^{2+} and Mg^{2+} cations were precipitated as carbonates. The ±0.1 difference from 1 may correspond to Na^+ impurities and can be within the error calculations. Under the preferential reaction conditions, a final product with a high carbonate purity (72%), rich in siderite ($FeCO_3$) (67%) was obtained. Furthermore, mild conditions that could be implemented in the industry were used.

Table 2. Final product composition showing carbonate purity (%), amount of $FeCO_3$ and $MgCO_3$ composing total amount of carbonates (%), Fe/Mg ratio, amount of silica (%), and stoichiometric results that verify results under each reaction condition (21, 60 and 80 °C), pH 9–12, and CO_2 mixture (10 vol.%).

T (°C)	pH	Reaction	% Carbonate (Purity)	% $FeCO_3$	% $MgCO_3$	Fe/Mg Ratio	% Silica	Stoichiometry
21	9	1	76.9	86.5	13.5	0.90	24.5	1.13
		2	77.2	93.7	6.3		22.7	1.16
		3	75.7	90.8	9.2		21.1	1.08
	10	1	75.7	82.9	17.1	0.85	21.1	1.05
		2	77.3	86.6	13.4		21.1	1.05
		3	78.6	85.9	14.1		20.5	1.03
	11	1	75.3	82.8	17.2	0.80	22.6	1.05
		2	71.2	78.6	21.4		15.5	0.98
		3	70.2	77.9	22.1		16.3	0.94
	12	1	70.6	74.3	25.7	0.74	18.7	0.94
		2	71.6	76.5	23.5		17.8	0.94
		3	72.1	72.1	27.9		16.5	0.87
60	9	1	72.0	90.2	9.8	0.83	19.3	1.11
		2	73.1	73.3	26.7		14.5	0.95
		3	69.4	84.8	15.2		17.8	1.02
	10	1	70.2	80.6	19.4	0.77	13.7	0.99
		2	68.6	77.3	22.7		13.9	0.96
		3	71.9	72.3	27.7		14.8	0.94
	11	1	69.4	73.9	26.1	0.71	16.2	0.95
		2	71.7	68.7	31.3		15.4	0.90
		3	69.1	69.1	30.9		13.2	0.91
	12	1	68.9	71.5	28.5	0.71	16.9	0.92
		2	70.0	73.4	26.6		14.2	0.95
		3	71.0	69.1	30.9		14.4	0.91
80	9	1	70.4	77.7	22.3	0.71	15.6	0.98
		2	69.1	68.9	31.1		11.0	0.95
		3	68.9	67.7	32.3		12.0	0.94
	10	1	72.8	68.7	31.3	0.68	15.2	0.93
		2	71.0	68.8	31.2		13.3	0.90
		3	73.5	68.0	32.0		14.3	0.92
	11	1	69.9	70.9	29.1	0.69	16.5	0.90
		2	68.9	68.0	32.0		12.2	0.93
		3	72.8	69.5	30.5		13.7	0.93
	12	1	71.7	67.7	32.3	0.68	14.9	0.91
		2	70.7	70.5	29.5		17.4	0.89
		3	72.0	67.1	32.9		14.1	0.91

3.3.3. Reaction Efficiency

The mineral carbonation reaction efficiency was calculated based on the CO_2 uptake per gram of initial residue (Table 3). Subsequently, the carbon storage potential of the mineral (mass of CO_2 that can be trapped in a unit mass of unreacted mineral) needed to be estimated following the equations proposed by Gadikota et al. [52]. The maximum storage capacity was estimated in 8.8 g CO_2. As expected, the most favorable results were obtained at pH 12 and 80 °C using 10 wt.% CO_2 after a reaction time of 2 h at ambient pressure, a stirring speed of 250 rpm, and a CO_2 injection rate of 1.5 L/min (0.15 L/min considering the 10 wt.% of CO_2 gas), with 0.125 ± 0.02 g CO_2 uptake/g solid and a reaction efficiency of 56.3 ± 6%. These reaction conditions were used to test the overall approach in a recirculation scenario.

Table 3. Mineral carbonation reaction efficiency using 10 vol.% CO_2 at different pH values (9–12) and temperatures (21, 60 and 80 °C). Values were calculated as arithmetic means of three recirculation reactions.

Temperature	pH	g CO_2 Uptake/g Residue	Reaction Efficiency (%)
21	9	0.011 ± 0.007	5.00 ± 0.8
	10	0.031 ± 0.02	14.1 ± 2
	11	0.039 ± 0.03	17.5 ± 3
	12	0.056 ± 0.03	37.4 ± 3
60	9	0.004 ± 0.008	2.01 ± 1
	10	0.012 ± 0.02	5.24 ± 1
	11	0.018 ± 0.02	8.25 ± 2
	12	0.045 ± 0.01	20.7 ± 4
80	9	0.002 ± 0.005	1.05 ± 0.8
	10	0.010 ± 0.01	4.66 ± 0.6
	11	0.042 ± 0.01	19.1 ± 4
	12	0.125 ± 0.02	57.3 ± 6

3.4. Global Mineral Carbonation Approach Evaluation

Once the most favorable reaction conditions had been optimized (pH 12, 80 °C, and 10 vol.% CO_2), they were used to evaluate the global technique considering the leaching and mineral carbonation reactions as previously described. Three recirculation reactions were carried out, reusing the recovered liquid (previous decrease in pH using NH_4HSO_4 as acid solvent) to perform the leaching stage. The overall process efficiency and mass and GHG balance were estimated. Finally, an overview of the global feasibility was done considering the possible valorization of the obtained products, the reuse of the reagents (2,2′-bipyridine and NH_4HSO_4), and possible solutions to replace NaOH as a basic solution for the pH-swinging process. Even though an exhaustive analysis was not done, the potential weak points regarding the industrial implementation of such a process were nonetheless identified.

3.4.1. Mass Balance

Based on the gas flow Equation (7), the leaching efficiency (Figures 4 and 5) and the ICP-OES, Total Inorganic Carbon and CHNS analysis performed before and after each step of the mineral carbonation process the mass balance have been estimated. Figure 8 shows the mass balance of each stage for the CO_2 and for both Fe^{2+} (as Fe_2O_3 and $[Fe(bipy)_3]^{2+}$) and Mg^{2+} cations (as MgO) for 4 g of initial mining residue treated in the whole process. Each balance summarizes the different reactions that have taken place until the final carbonate precipitation with the optimized reaction conditions as presented in the process schema (Figure 2). The mass balance calculations include the three leaching processes making the different between the first with pure NH_4HSO_4 and the second and third when the iron was already complexed, the iron complexation with 2,2′-bipyridine and the total balance for the three mineral carbonation reactions identified as R1, R2 and R3. The leaching mass balances show the difference between the Fe and Mg leached at the initial leaching and when the recovered liquid is used. The mass balances were calculated based on the leaching results obtained in the laboratory assays. The most important information obtained from these mass balances is the possibility of total reuse of the ligand 2,2′-bipyridine and the decrease in the amount of NH_4HSO_4 needed to perform the 2nd and the 3rd leaching process. While 20 g of the NH_4HSO_4 aqueous solution is needed to perform the 1st leaching process, 4 additional grams is required to carry out the 2nd and the 3rd leaching, decreasing the amount 10 times, leading to a substantial reduction of the total cost if it is carried out on an industrial scale.

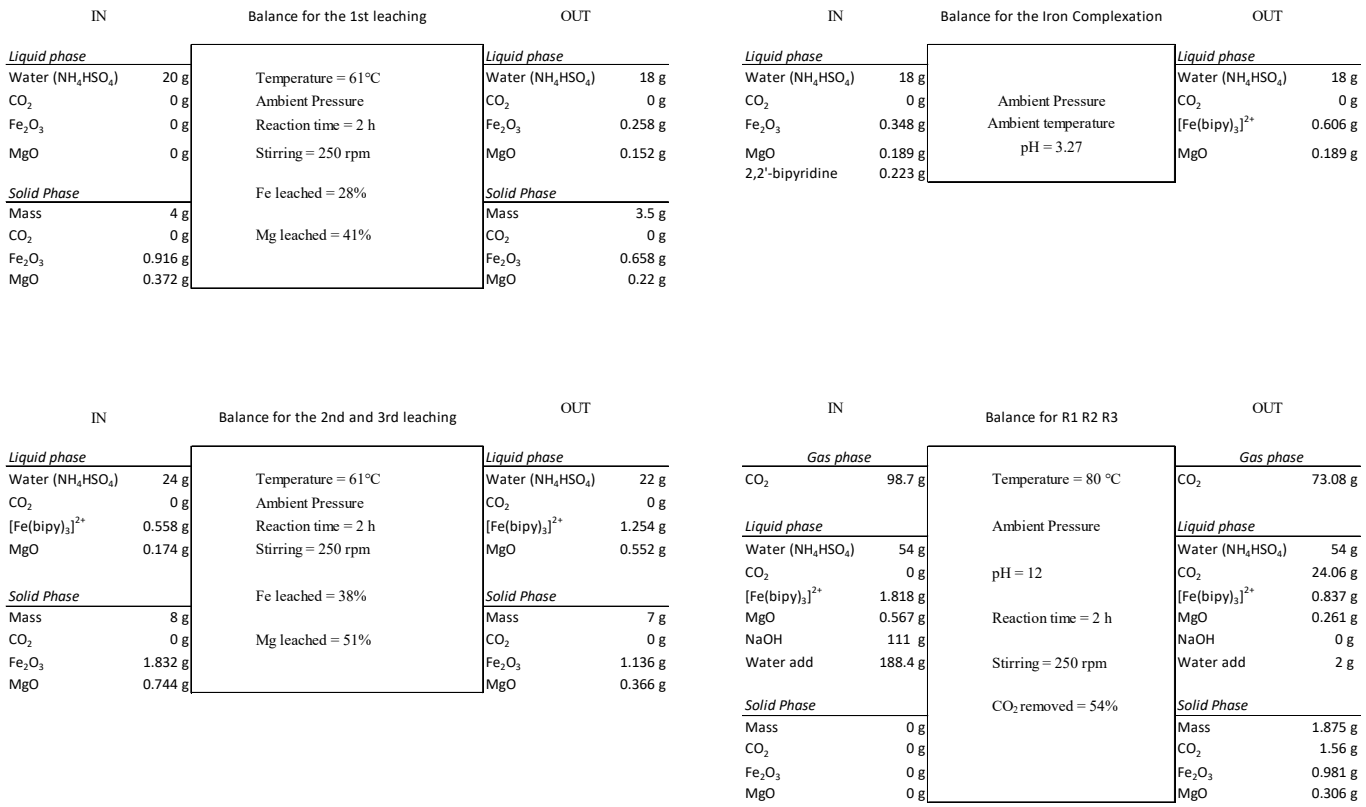

Figure 8. Global process mass balance for each recirculation process (R1, R2, R3) calculated for 4 g of initial residue.

The gas flow rate is 1.5 L/min knowing that the CO_2 rate is 10%, 0.15 L/min of CO_2. At atmospheric pressure and T = 20 °C and according to Equation (7) the mass of CO_2 is as follows:

$$m_{CO2} = \frac{P * V}{R * T} * MCO_2 = \frac{1.013 * 10^5 * 0.15 * 10^{-3}}{8.32 * 293} * 44 = 0.2742\ g{\cdot}CO_2/min \quad (7)$$

Three mineral carbonation processes were done using 32.9 g of gas during each reaction, so 98.7 g of CO_2 is used across R1, R2 and R3. The amount of CO_2, Fe_2O_3, $[Fe(bipy)_3]^{2+}$ and MgO in the liquid and solid phases were calculated based on the reaction efficiency observed during the laboratory assays. The net amount of CO_2 removed from the flue gas is just 28 wt.%, while the 72 wt.% is not dissolved and does not take place in the reaction, so decrease in the CO_2 gas flow could be done in order to optimize the overall process. The CO_2 present in the solid phase (CO_2 store) leading to a 54% of reaction efficiency is we only take into account the mineral carbonation reaction. As the reactions are taken place at 80 °C and ambient pressure, the volume increases cause by the addition of NaOH and NH_4HSO_4 could be controlled by evaporation. The amounts of Si, Ca and Na present in the solid phase are not counted because they do not lead to carbonate precipitation.

The overall mass balance is presented in Figure 9. Estimations were done considering 1 ton of initial residue. Given that 38% and 51% of Fe^{2+} and Mg^{2+} were leached, a total of 236 Kg of Fe-rich carbonates are precipitated. The amount of CO_2, $[Fe(bipy)_3]^{2+}$ and MgO still present in the liquid phase are 2000, 69 and 21 kg, respectively. The overall process efficiency was estimated at 130 $KgCO_2/t$ of initial residue. As the total volume could be controlled by evaporation, the model can consider the recirculation of water.

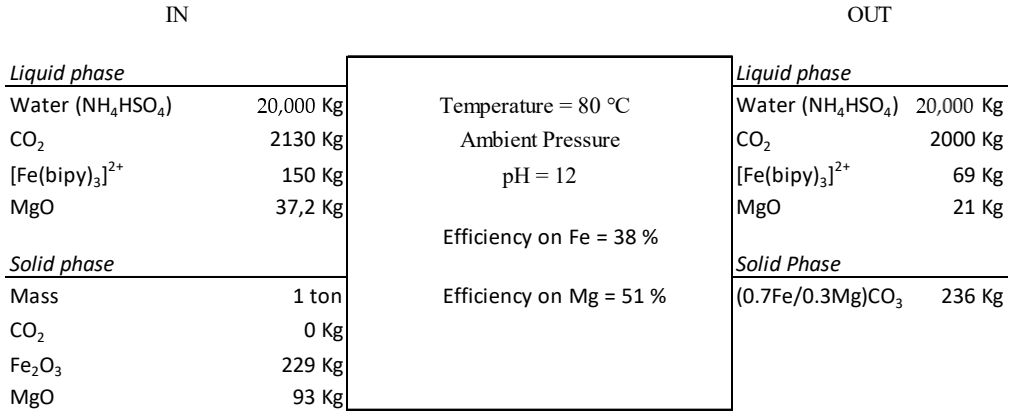

Figure 9. Overall process mass balance estimated for 1 ton of initial residue.

3.4.2. Global Reaction Efficiency

Based on the results described and discussed in previous sections and to verify the effectiveness of the proposed mineral carbonation technique, the global reaction efficiency was estimated. For this purpose, three recirculation reactions were carried out. When the global technique efficiency was calculated, the amount of CO_2 precipitated in the solid phase was viewed as CO_2 removed. In light of the mineral carbonation results in Section 3.3.3, the results showed consistent values of 0.52 ± 0.06 g of CO_2 uptake for each mineral carbonation reaction, which amounted to approximately 1.56 g of CO_2 uptake after three successive recirculation reactions. Considering that 4 g of mining residue was used for each recirculation reaction, the amount of CO_2 removed per gram of residue was calculated, showing an initial residue of 0.13 ± 0.04 g CO_2/g (Figure 10). Following the equations and calculations performed by Gadikota, Swanson, Zhao and Park [53], the maximum CO_2 storage capacity of the reaction was estimated in 0.88 g of CO_2 for each recirculation reaction. Using this value, the mineral carbonation reaction efficiency was calculated, showing that 57.3 ± 6% of CO_2 was removed. However, considering both the leaching of Fe and Mg cations and the mineral carbonation reaction efficiency, the overall approach efficiency was 24 ± 6% in terms of residue conversion to a iron-rich carbonate. The global reaction efficiency could be substantially increased if the possible recovery potential of the mining residue was considered, where, after three leaching processes, almost all Fe and Mg were leached and 12% and 2% of the cations remained, respectively. This led to an overall efficiency of around 50% in carbonate conversion. A more detailed study should be done to determine the feasibility of the system at a larger scale.

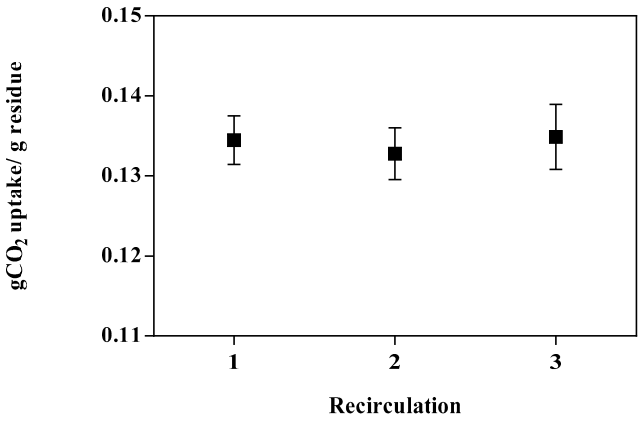

Figure 10. Overall technique efficiency for each recirculation reaction calculated as g CO_2 uptake/g residue considering both leaching and mineral carbonation reaction efficiency. Reactions occurred at atmospheric pressure, 250 rpm, pH 12, 80 °C, and 10 vol.% CO_2 for reaction time of 2 h. Error bars indicate 5% error; n = 3.

It can be concluded that the results obtained in this process using mild reaction conditions were high compared with previous fayalite mineral carbonation studies [32,54–56].

3.5. GHG Balance

The overall GHG balance determined the direct environmental impact of the mineral carbonation reaction, and the integrity of the proposed CO_2 sequestration approach could be verified. The impacts of the residue transportation and overall energy requirements were used to estimate the generated CO_2 equivalent emissions. Since the leaching stages and mineral carbonation reactions did not require very high temperatures, GHG emissions are low. The main source of GHG emissions come from the transportation from Mine Arnaud to the mineral carbonation plant near the industrial emitters (ArcelorMittal and Aluminerie Alouette Inc., Sept-Îles, QC, Canada). Nevertheless, the distance was near, and the energy requirements were not likely to be very high. Trucks and trains are the only two only means of land transportation, and the emission factor of road transportation is half that of rail (0.07 vs. 0.12) Pasquier, Mercier, Blais, Cecchi and Kentish [8]. However, the Sept-Îles region does not have a railway line connecting Mine Arnaud and the above-mentioned industrial emitters, and trucks are the only available land transportation. The transportation of mining residues by diesel trucks represents a total of 3.07 and 6.34 kg of CO_2 eq/ton of residues, respectively, for the distances of 15 km to Aluminerie Alouette and 31 km to ArcelorMittal. Using other fuels, such as biodiesel, natural gas, ethanol, or hybrid fuels (biodiesel/diesel B20), could reduce GHG emissions. However, many trips would be required for the daily transportation of all the mining residues, which would significantly increase the GHG emissions. Due to the large residue volumes that must be transported, shipping would be the most appropriate option. The use of a conveyor might also be a viable transportation option between Mine Arnaud and Aluminerie Alouette because of their proximity (~15 km); although there would be additional construction and maintenance costs, the GHG emissions could be reduced.

Since the particle size of the mine tailings was already optimal, no crushing was required. The leaching and mineral carbonation reaction were powered by electricity, the emission factor of which is 2.5 g CO_2 eq/kWh in Quebec [57]. Estimations suggested that 1.92 kg CO_2/ton of residues would be emitted. These emissions were related to the water heating required for the leaching (60 °C) and mineral carbonation reaction (80 °C), the emissions of which were estimated to be 0.58 and 1.22 kg CO_2/ton of residue, respectively. The GHG emissions related to the other steps of this approach were considered negligible. The global emissions were estimated to be 11.33 kg CO_2/ton of residue. Considering that 130 kg CO_2/ton of residue was sequestered in the overall reaction (Section 3.3.2), the GHG balance was positive in terms of CO_2 removed. Nevertheless, these data were approximate, and more in-depth research is necessary. An exhaustive economic study is also necessary to evaluate the feasibility of the proposed approach for industrial implementation.

4. Conclusions

The feasibility of an indirect mineral carbonation technique for post-combustion CO_2 sequestration by iron complexation using 2,2′-bipyridine was evaluated. This study focused on finding the preferential parameters of the overall approach in a recirculation scenario. First, in the leaching stage, 38 and 51% of Fe and Mg cations were leached. The possible valorization of the product obtained was also reported. It was demonstrated that 87% of the cations were leached after three leaching stages. A residue with a silica purity of 87% with potential sale value was obtained.

Subsequently, the mineral carbonation reaction and prior complexation of Fe^{2+} with 2,2′-bipyridine were studied in a recirculation scenario after three reaction batches. The study confirmed the total recovery potential of the 2,2′-bipyridine, which could significantly decrease the overall cost of the mineral carbonation approach. Furthermore, the most favorable reaction conditions were at a pH of 12, a temperature of 80 °C, and ambient pressure after a reaction time of 2 h and using 10% vol. CO_2 gas. A stable carbonate

(0.7 Fe/0.3 $MgCO_3$) was formed with a purity of 71% and a reaction efficiency of 57.3%. Under these conditions, a global approach evaluation was performed. It was confirmed that 0.13 g CO_2/g initial residue could be removed with an efficiency of 24%. This value could be increased up to 50% if the valorization of the mining residue was considered. Furthermore, the NH_4HSO_4 used to regulate the pH was decreased five-fold.

Finally, the GHG balance was estimated. Firstly, 130 kg CO_2/ton of residue could be removed, yielding 236 kg of Fe-rich carbonate. Secondly, no pre-treatment, heat activation, or grinding was needed, the transportation distances of the solid residue were short, and the reactions could be powered by hydroelectric energy, realizing a global emission estimation of 11.33 kg CO_2/ton of residue. Nevertheless, an exhaustive economic and energetic study should be done.

This study further confirmed the possibility of performing mineral carbonation using Fe-rich mining residues and post-combustion industrial CO_2 gas in a recirculation scenario. Although the proposed approach was performed in the Sept-Îles region (Sept-Îles, QC, Canada) using Mine Arnaud mining residue, it provides guidance for the development of mineral carbonation by cation complexation using iron-rich olivine as a viable sequestration technique in other regions. This is mostly because only mild conditions were necessary for the proposed approach, in contrast to previous studies, where strong conditions were used that made industrial implementation unfeasible.

Author Contributions: Conceptualization, J.F.R., G.M., J.-F.B. and L.-C.P.; methodology, J.F.R., G.M., J.-F.B. and L.-C.P.; validation, J.F.R., G.M., J.-F.B. and L.-C.P.; formal analysis, J.F.R.; investigation, J.F.R., G.M., J.-F.B. and L.-C.P.; resources, J.F.R., G.M., J.-F.B. and L.-C.P.; data curation, J.F.R., G.M., J.-F.B. and L.-C.P.; writing—original draft preparation, J.F.R.; writing—review and editing, G.M., J.-F.B. and L.-C.P.; visualization, J.F.R., G.M., J.-F.B. and L.-C.P.; supervision, G.M., J.-F.B. and L.-C.P.; project administration, J.F.R., G.M., J.-F.B. and L.-C.P.; funding acquisition, G.M., J.-F.B. and L.-C.P. All authors have read and agreed to the published version of the manuscript.

Funding: This research was funded by Fonds Québecois pour la Recherche et les Technologies (FQRNT), Programme de recherche en partenariat sur le développement durable du secteur minier, grant number 2017-MI-202241.

Institutional Review Board Statement: Not applicable.

Informed Consent Statement: Not applicable.

Data Availability Statement: Not applicable.

Acknowledgments: I acknowledge all the support given for the production of this article including the administrative and technical support.

Conflicts of Interest: The authors declare no conflict of interest. The funders had no role in the design of the study; in the collection, analyses, or interpretation of data; in the writing of the manuscript, or in the decision to publish the results.

References

1. Shukla, P.; Skea, J.; Calvo Buendia, E.; Masson-Delmotte, V.; Pörtner, H.; Roberts, D.; Zhai, P.; Slade, R.; Connors, S.; Van Diemen, R. *IPCC, 2019: Climate Change and Land: An IPCC Special Report on Climate Change, Desertification, Land Degradation, Sustainable Land Management, Food Security, and Greenhouse Gas Fluxes in Terrestrial Ecosystems*; IPCC: Geneva, Switzerland, 2019.
2. IPCC. *Annex III, Working Group III Contribution to the IPCC 5th Assessment Report "Climate Change 2014: Mitigation of Climate Change"*; IPCC: Geneva, Switzerland, 2014; p. 46.
3. Hansen, J.; Sato, M.; Hearty, P.; Ruedy, R.; Kelley, M.; Masson-Delmotte, V.; Russell, G.; Tselioudis, G.; Cao, J.; Rignot, E. Ice melt, sea level rise and superstorms: Evidence from paleoclimate data, climate modeling, and modern observations that 2 °C global warming is highly dangerous. *Atmos. Chem. Phys. Discuss.* **2015**, *15*, 1680–7367.
4. Dow, K.; Downing, T.E. *The Atlas of Climate Change: Mapping the World's Greatest Challenge*; University of California Press: Berkeley, CA, USA, 2016; p. 0520966821.
5. Jones, M.C.; Cheung, W.W. Multi-model ensemble projections of climate change effects on global marine biodiversity. *ICES J. Mar. Sci.* **2015**, *72*, 741–752. [CrossRef]

6. IPCC. *Global Warming of 1.5 °C, an IPCC Special Report on the Impacts of Global Warming of 1.5 °C above Pre-Industrial Levels and Related Global Greenhouse Gas Emission Pathways, in the Context of Strengthening the Global Response to the Threat of Climate Change, Sustainable Development, and Efforts to Eradicate Poverty*; IPCC: Geneva, Switzerland, 2018.
7. Western Climate Initiative (WCI). Cadre de Mise en Oeuvre du Programme Régional de la Western Climate Initiative (WCI). Available online: http://www.westernclimateinitiative.org/the-wci-cap-and-trade-program/program-design (accessed on 27 March 2020).
8. Pasquier, L.-C.; Mercier, G.; Blais, J.-F.; Cecchi, E.; Kentish, S. Technical & economic evaluation of a mineral carbonation process using southern Québec mining wastes for CO_2 sequestration of raw flue gas with by-product recovery. *Int. J. Greenh. Gas Control* **2016**, *50*, 147–157. [CrossRef]
9. ECRA. Deployment of CO_2 Capture in the Cement Industry. In Proceedings of the CCS-Conference, Brevik, Norway, 20–21 May 2015.
10. Arts, R.; Chadwick, A.; Eiken, O.; Thibeau, S.; Nooner, S. Ten years' experience of monitoring CO_2 injection in the Utsira Sand at Sleipner, offshore Norway. *First Break* **2008**, *26*, 1365–2397. [CrossRef]
11. Leeson, D.; Mac Dowell, N.; Shah, N.; Petit, C.; Fennell, P.S. A Techno-economic analysis and systematic review of carbon capture and storage (CCS) applied to the iron and steel, cement, oil refining and pulp and paper industries, as well as other high purity sources. *Int. J. Greenh. Gas Control* **2017**, *61*, 71–84. [CrossRef]
12. Romanov, V.; Soong, Y.; Carney, C.; Rush, G.E.; Nielsen, B.; O'Connor, W. Mineralization of carbon dioxide: A literature review. *ChemBioEng Rev.* **2015**, *2*, 231–256. [CrossRef]
13. Rahmani, O.; Junin, R.; Tyrer, M.; Mohsin, R. Mineral carbonation of red gypsum for CO_2 sequestration. *Energy Fuels* **2014**, *28*, 5953–5958. [CrossRef]
14. Seifritz, W. CO_2 disposal by means of silicates. *Nature* **1990**, *345*, 486. [CrossRef]
15. Dunsmore, H. A geological perspective on global warming and the possibility of carbon dioxide removal as calcium carbonate mineral. *Energy Convers. Manag.* **1992**, *33*, 565–572. [CrossRef]
16. Lackner, K.S.; Wendt, C.H.; Butt, D.P.; Joyce, B.L.; Sharp, D.H. Carbon dioxide disposal in carbonate minerals. *Energy* **1995**, *20*, 1153–1170. [CrossRef]
17. Lackner, K.S.; Butt, D.P.; Wendt, C.H. Progress on binding CO_2 in mineral substrates. *Energy Convers. Manag.* **1997**, *38*, S259–S264. [CrossRef]
18. Turianicová, E.; Baláž, P.; Tuček, Ľ.; Zorkovská, A.; Zeleňák, V.; Németh, Z.; Šatka, A.; Kováč, J. A comparison of the reactivity of activated and non-activated olivine with CO_2. *Int. J. Miner. Process.* **2013**, *123*, 73–77. [CrossRef]
19. Johnson, N.C.; Thomas, B.; Maher, K.; Rosenbauer, R.J.; Bird, D.; Brown, G.E. Olivine dissolution and carbonation under conditions relevant for in situ carbon storage. *Chem. Geol.* **2014**, *373*, 93–105. [CrossRef]
20. Kemache, N.; Pasquier, L.-C.; Mouedhen, I.; Cecchi, E.; Blais, J.-F.; Mercier, G. Aqueous mineral carbonation of serpentinite on a pilot scale: The effect of liquid recirculation on CO_2 sequestration and carbonate precipitation. *Appl. Geochem.* **2016**, *67*, 21–29. [CrossRef]
21. Béarat, H.; McKelvy, M.J.; Chizmeshya, A.V.G.; Gormley, D.; Nunez, R.; Carpenter, R.W.; Squires, K.; Wolf, G.H. Carbon sequestration via aqueous olivine mineral carbonation: Role of passivating layer formation. *Environ. Sci. Technol.* **2006**, *40*, 4802–4808. [CrossRef] [PubMed]
22. Rahmani, O.; Highfield, J.; Junin, R.; Tyrer, M.; Pour, A.B. Experimental investigation and simplistic geochemical modeling of CO2 mineral carbonation using the mount tawai peridotite. *Molecules* **2016**, *21*, 353. [CrossRef]
23. Pasquier, L.-C. *Procédé de Piegeage du CO_2 Industriel par Carbonatation Minérale de Résidus Miniers Silicatés (Serpentinite) et Valorisation des Sous-Produits*; Institut National de la Recherche Scientifique: Québec, QC, Canada, 2014.
24. Sanna, A.; Steel, L.; Maroto-Valer, M.M. Carbon dioxide sequestration using NaHSO4 and NaOH: A dissolution and carbonation optimisation study. *J. Environ. Manag.* **2017**, *189*, 84–97. [CrossRef]
25. Werner, M.; Hariharan, S.; Mazzotti, M. Flue gas CO_2 mineralization using thermally activated serpentine: From single-to double-step carbonation. *Phys. Chem. Chem. Phys.* **2014**, *16*, 24978–24993. [CrossRef]
26. Farhang, F.; Oliver, T.; Rayson, M.; Brent, G.; Stockenhuber, M.; Kennedy, E. Experimental study on the precipitation of magnesite from thermally activated serpentine for CO_2 sequestration. *Chem. Eng. J.* **2016**, *303*, 439–449. [CrossRef]
27. Kashim, M.Z.; Tsegab, H.; Rahmani, O.; Abu Bakar, Z.A.; Aminpour, S.M. Reaction Mechanism of Wollastonite In Situ Mineral Carbonation for CO_2 Sequestration: Effects of Saline Conditions, Temperature, and Pressure. *ACS Omega* **2020**, *5*, 28942–28954. [CrossRef]
28. Haque, F.; Santos, R.M.; Chiang, Y.W. CO_2 sequestration by wollastonite-amended agricultural soils–An Ontario field study. *Int. J. Greenh. Gas Control* **2020**, *97*, 103017. [CrossRef]
29. Ayub, S.A.; Tsegab, H.; Rahmani, O.; Beiranvand Pour, A. Potential for CO_2 Mineral Carbonation in the Paleogene Segamat Basalt of Malaysia. *Minerals* **2020**, *10*, 1045. [CrossRef]
30. Daval, D.; Martinez, I.; Corvisier, J.; Findling, N.; Goffe, B.; Guyot, F. Carbonation of Ca-bearing silicates, the case of wollastonite: Experimental investigations and kinetic modeling. *Chem. Geol.* **2009**, *265*, 63–78. [CrossRef]
31. Zhang, J.S.; Zhang, R.; Geerlings, H.; Bi, J.C. A Novel Indirect Wollastonite Carbonation Route for CO_2 Sequestration. *Chem. Eng. Technol.* **2010**, *33*, 1177–1183. [CrossRef]
32. Qafoku, O.; Kovarik, L.; Kukkadapu, R.K.; Ilton, E.S.; Arey, B.W.; Tucek, J.; Felmy, A.R. Fayalite dissolution and siderite formation in water-saturated supercritical CO_2. *Chem. Geol.* **2012**, *332–333*, 124–135. [CrossRef]

33. Penner, L.; O'Connor, W.K.; Dahlin, D.C.; Gerdemann, S.; Rush, G.E. *Mineral Carbonation: Energy Costs of Pretreatment Options and Insights Gained from Flow Loop Reaction Studies*; Albany Research Center, Office of Fossil Energy, US DOE: Albany, OR, USA, 2004; p. 18.
34. Qafoku, O.; Ilton, E.S.; Bowden, M.E.; Kovarik, L.; Zhang, X.; Kukkadapu, R.K.; Engelhard, M.H.; Thompson, C.J.; Schaef, H.T.; McGrail, B.P.; et al. Synthesis of nanometer-sized fayalite and magnesium-iron(II) mixture olivines. *J. Colloid Interface Sci.* **2018**, *515*, 129–138. [CrossRef]
35. Li, J.; Hitch, M. A Review on Integrated Mineral Carbonation Process in Ultramafic Mine Deposit. *Geo-Resour. Environ. Eng. (GREE)* **2017**, *2*, 148–154. [CrossRef]
36. Rahmani, O. CO_2 sequestration by indirect mineral carbonation of industrial waste red gypsum. *J. CO_2 Util.* **2018**, *27*, 374–380. [CrossRef]
37. Mine Arnaud. Groupe-conseil, Consultants externes, Roche ltée and Ausenco Sandwell. In *Projet Minier Arnaud—Étude d 'Impact sur l 'Environnement*; Mine Arnaud: Sept-Îles, QC, Canada, 2012; p. 726.
38. Ministère du Développement Durable, d.l.E.e.d.l.L.c.l.c.c. Émissions de gaz à Effet de Serre Déclarées et Vérifiées des Établissements Visés par le Règlement Concernant le Système de Plafonnement et D'échange de Droits D'émission de gaz à Effet de Serre (RSPEDE). Available online: http://www.mddelcc.gouv.qc.ca/changements/carbone/ventes-encheres/liste-etablissements-visesRSPEDE.pdf (accessed on 13 October 2017).
39. Gerbet, T. (Ed.) *Gaz à Effet de Serre: La Carte des Émissions Industrielles au Québec*; Radio-Canada: Toronto, ON, Canada, 2014.
40. Tanupabrungsun, T.; Young, D.; Brown, B.; Nešic, S. Construction and verification of pourbaix diagrams for CO_2 corrosion of mild steel valid up to 250 °C. In Proceedings of the CORROSION, Salt Lake City, UT, USA, 11–15 March 2012.
41. Den Boef, G.; Zuur, A.P. *Theoretische Grondslagen van de Analyse in Waterige Oplossingen*; Elsevier: Amsterdam, The Netherlands, 1980; p. 9010103730.
42. Josceanu, A.M.; Moore, P. Comparison of the rates and mechanisms of formation and solvolysis of $[Fe(bipy)_3]^{2+}$ (bipy = 2,2′-bipyridine) and $[FeL]^{2+}$ [L = 1,4,7-tris(2,2′-bipyridyl-5-ylmethyl)-1,4,7-triazacyclononane] and their stabilities in dimethylformamide solution. *J. Chem. Soc. Dalton Trans.* **1998**, *24*, 369–374. [CrossRef]
43. Pasquier, L.-C.; Mercier, G.; Blais, J.-F.; Cecchi, E.; Kentish, S. Parameters optimization for direct flue gas CO_2 capture and sequestration by aqueous mineral carbonation using activated serpentinite based mining residue. *Appl. Geochem.* **2014**, *50*, 66–73. [CrossRef]
44. Sanna, A.; Lacinska, A.; Styles, M.; Maroto-Valer, M.M. Silicate rock dissolution by ammonium bisulphate for pH swing mineral CO2 sequestration. *Fuel Process. Technol.* **2014**, *120*, 128–135. [CrossRef]
45. Office de L'éfficacité Énérgétique. *Annexe B Coefficient D'émission de CO_2*; Office de L'éfficacité Énérgétique: Québec, QC, Canada, 2018.
46. Khattak, R.; Naqvi, I.I. Addition product of iron (II) complex of aromatic diimine with sulphuric acid. *J. Res. (Sci.)* **2007**, *18*, 219–235.
47. Tangstad, M. Ferrosilicon and silicon technology. In *Handbook of Ferroalloys*; Elsevier: Amsterdam, The Netherlands, 2013; pp. 179–220. [CrossRef]
48. Gasik, M. *Handbook of Ferroalloys: Theory and Technology*; Butterworth-Heinemann: Oxford, UK, 2013; p. 0080977669.
49. Patnaik, P. *Dean's Analytical Chemistry Handbook*; McGraw-Hill: New York, NY, USA, 2004; Volume 1143.
50. Gunning, P.J.; Hills, C.D.; Carey, P.J. Accelerated carbonation treatment of industrial wastes. *Waste Manag. (Oxford)* **2010**, *30*, 1081–1090. [CrossRef]
51. Haynes, W.M. *CRC Handbook of Chemistry and Physics*; CRC Press: Boca Raton, FL, USA, 2014; p. 1482208687.
52. Schott, J.; Mavromatis, V.; Fujii, T.; Pearce, C.R.; Oelkers, E.H. The control of magnesium aqueous speciation on Mg isotope composition in carbonate minerals: Theoretical and experimental modeling. *Chem. Geol.* **2016**, *445*, 120–134. [CrossRef]
53. Gadikota, G.; Swanson, E.J.; Zhao, H.; Park, A.-H.A. Experimental Design and Data Analysis for Accurate Estimation of Reaction Kinetics and Conversion for Carbon Mineralization. *Ind. Eng. Chem. Res.* **2014**, *53*, 6664–6676. [CrossRef]
54. Mora Mendoza, E.Y.; Sarmiento Santos, A.; Vera López, E.; Drozd, V.; Durygin, A.; Chen, J.; Saxena, S.K. Siderite Formation by Mechanochemical and High Pressure–High Temperature Processes for CO_2 Capture Using Iron Ore as the Initial Sorbent. *Processes* **2019**, *7*, 735. [CrossRef]
55. Llorens, I.; Fattahi, M.; Grambow, B. New synthesis route and characterization of siderite ($FeCO_3$) and coprecipitation of 99Tc. *MRS Online Proc. Libr. Arch.* **2006**, *985*, 1208. [CrossRef]
56. Lammers, K.; Murphy, R.; Riendeau, A.; Smirnov, A.; Schoonen, M.A.A.; Strongin, D.R. CO_2 Sequestration through Mineral Carbonation of Iron Oxyhydroxides. *Environ. Sci. Technol.* **2011**, *45*, 10422–10428. [CrossRef]
57. Environment and Climate Change Canada. Canadian Environmental Sustainability Indicators: Greenhouse Gas Emissions. Available online: www.ec.gc.ca/indicateurs-indicators/default.asp?lang=En&n=FBF8455E-1 (accessed on 16 October 2017).